The $^{16}O(\vec{\gamma},\pi^- p)$ reaction at $E_\gamma \simeq 300$ MeV

K. Hicks,[2] V. Gladyshev,[5] H. Baghaei,[5] A. Caracappa,[1] A. Cichocki,[5] R. Deininger,[2] R. Finlay,[2] T. Gresko,[5] S. Hoblit,[1] M. Khandaker,[6] O. Kistner,[1] F. X. Li,[4] R. Lindgren,[5] M. Lucas,[3] L. Miceli,[1] B. Norum,[5] J. Rapaport,[2] A. Sandorfi,[1] R. Sealock,[5] L. C. Smith,[5] C. Thorn,[1] S. Thornton,[5] C. S. Whisnant,[3] D. Willits,[2] and L. E. Wright[2]

[1]*Physics Department, Brookhaven National Laboratory, Upton, New York 11973*

[2]*Department of Physics and Astronomy, Ohio University, Athens, Ohio 45701*

[3]*Department of Physics, University of South Carolina, Columbia, South Carolina 29208*

[4]*Department of Physics, George Washington University, Washington, D.C. 20052*

[5]*Department of Physics, University of Virginia, Charlottesville, Virginia 22903*

[6]*Physics Department, Virginia Polytechnic Institute & State University, Blacksburg, Virginia 24061*

(Received 26 October 1999; published 7 April 2000)

Cross sections are presented for the $^{16}O(\vec{\gamma},\pi^- p)$ reaction at incident photon energies between 290 and 325 MeV. The data are presented for specific proton and pion angles as a function of proton energy, which are compared with calculations in a local distorted wave impulse approximation model. The results are in agreement at most kinematics, although at some kinematics the data and calculations disagree by a factor of 2 or more. These data do not support the conclusion of a large modification to the mass of the Δ resonance in the nucleus.

PACS number(s): 25.20.Lj, 13.60.Le, 24.70.+s, 14.20.Gk

I. INTRODUCTION

Measurements of pion photoproduction have been carried out on both nucleon and nuclear targets for many years [1]. A primary goal of these studies has been to understand the dynamics that result in the creation of a pion from the energy provided by the photon. In most theoretical models, the Δ resonance at 1232 MeV with a width of about 120 MeV plays a key role. At photon energies near 300 MeV, the dominant mechanism is absorption on the nucleon by a magnetic dipole ($M1$) interaction, causing a spin flip of one of the quarks resulting in the Δ resonance. Multipoles other than $L=0$ also contribute, but to a lesser degree.

An understanding of the ΔN interaction is essential to the dynamics of many phenomena ranging from pion photoproduction to the nucleon-nucleon interaction. The NN interaction has diagrams that include ΔN terms at center of mass energies of 300 MeV. Data on photodisintegration of the deuteron at energies near the 300 MeV are sensitive to the ΔN interaction in calculations [2]. New information on the ΔN interaction will help guide theoretical models.

The goal of the present measurement is to learn how the Δ resonance interacts with other nucleons in the nucleus. In particular, the theoretical calculations in the model of Lee, Wright, and Bennhold [3] suggest that the $(\gamma,\pi^- p)$ reaction should be sensitive to the ΔN interaction. Previous measurements [4] of $^{16}O(\vec{\gamma},\pi^- p)$ at $E_\gamma = 360$ MeV report cross sections a factor of 4 smaller than the calculations. By reducing the mass of the delta resonance by 5% in the calculations [3], as an approximation to including a scalar potential for the Δ in the nucleus [5], much better agreement with this data is obtained. While this alone is not conclusive evidence for the ΔN potential, it does show the sensitivity of these data to the ΔN interaction. Empirical data with better statistical precision for pion photoproduction from nuclear targets are needed in order to motivate more detailed theoretical calculations with explicit inclusion of ΔN interaction terms.

We report here cross sections for the $^{16}O(\vec{\gamma},\pi^- p)$ reaction at photon energies of 290–325 MeV and compare the results with theoretical calculations. In Sec. II, the theoretical model is discussed. In Sec. III, a more detailed discussion of previous measurements is presented. Details of the kinematics and a description of the experimental setup for the present measurement are given in Sec. IV. Data are presented at proton angles of 55° and 75° and a corresponding range of pion angles from 36° to 140° in 8° steps. This choice of kinematics spans the peak of the quasifree cross section in the best way possible for our experimental setup. A comparison of these data and calculations is given in Sec. V, and conclusions are drawn in Sec. VI.

II. THEORETICAL MODEL

The calculations used here are based on the model of Lee, Wright, and Bennhold [3] for the reaction $A(\gamma,\pi N)B$. The basic idea of the model is an impulse approximation where the incoming photon of momentum $\mathbf{k}$ strikes a bound nucleon with momentum $\mathbf{p}_i$ and produces a pion of momentum $\mathbf{q}'$ and a residual nucleon with momentum $\mathbf{p}'$. As the pion and nucleon exit the nucleus they interact with the remaining nucleons via optical potentials which change the momenta $\mathbf{q}'$ and $\mathbf{p}'$ to their asymptotic values $\mathbf{q}$ and $\mathbf{p}$. Thus there are three basic ingredients: (1) single nucleon bound-state wave functions and associated spectroscopic factors, (2) the elementary pion photoproduction operator, and (3) pion and nucleon optical potentials. The energies of the asymptotic particles are E_γ for the incoming photon, E_π for the outgoing pion, E_N for the outgoing nucleon, and M_i for the initial nucleus. The final nucleus has rest mass M_f (which includes the change in binding energy for the particle knocked out) plus kinetic energy $T_Q = \mathbf{Q}^2/2M_f$ where $\mathbf{Q}$ is the recoil momentum of the final nucleus and is given by

$\mathbf{Q}=\mathbf{k}-\mathbf{q}-\mathbf{p}$. Overall energy conservation gives $E_\gamma+M_i=E_\pi+E_N+M_f+T_Q$. To conserve energy and momentum at the vertex, the model uses the impulse approximation which requires that the momentum of the struck nucleon is equal to the negative of the momentum transfer $\mathbf{p}_i=-\mathbf{Q}$.

Harmonic oscillator wave functions are used for the bound nucleons and the complete Blomqvist-Laget pion production operator [6–9] is used for the elementary operator. This operator is based on a Feynman diagram approach which includes the Born terms and the Δ resonance. (See Ref. [3] for complete details.) The operator is expressed in an arbitrary frame of reference which is convenient since the bound nucleon has a distribution of momentum. Furthermore, the pion photoproduction operator depends strongly on the momenta of the particles at the vertex, so in an *r*-space evaluation of the matrix element it is nonlocal. The calculation uses the pion optical model developed by Stricker, McManus, and Carr [10] whose parameters were fitted to low-energy data and then extrapolated up to 220 MeV, giving reasonable agreement with experimental data. The global phenomenological potential of Schwandt *et al.* [11] is used for the nucleon optical potential, which is valid for nucleons with kinetic energy below 200 MeV.

The model contains various levels of approximation. One is the plane wave approximation where the outgoing pion and nucleon are given by plane waves. In this approximation, the spatial matrix element is a Fourier transform of the bound nucleon wave function. With the optical potentials active, one can perform a local calculation referred to as the local distorted wave impulse approximation (local DWIA) where the intermediate momenta $\mathbf{q}'$ and $\mathbf{p}'$ are fixed at their asymptotic values of $\mathbf{q}$ and $\mathbf{p}$, respectively. Within the DWIA formalism, the optical potentials model the final state interactions of the outgoing proton and pion. Finally one can perform the full nonlocal calculation in momentum space which involves evaluating a six-dimensional integral numerically. Under kinematic conditions involving large momentum transfers, the nonlocalities can be significant (of order 20–30 %), but for most kinematics where the cross section is large the local DWIA calculation is sufficient. All the results in this paper are calculated using the local DWIA.

The calculations include spectroscopic factors for each shell (the $p_{1/2}$, $p_{3/2}$, and the $s_{1/2}$). The spectroscopic factor is an overall scale factor for each shell that includes two factors, one is the occupation probability for that shell and the second is the overlap integral of the $A-1$ target nucleons not involved in the reaction with the residual nucleus. In general we do not attempt to evaluate these two factors separately, but rather use values determined experimentally from $(e,e'p)$ reactions from the same target nucleus [12,13]. For the case of ^{16}O the values for the spectroscopic factor are near 60% for the $p_{3/2}$ and $p_{1/2}$ shells. The deeper $s_{1/2}$ shell is spread out over energy and not so clearly determined. Because the spectroscopic factors are not precisely determined from experiments, there is an overall uncertainty of about 10% in the absolute normalization of the calculations.

For the particular reaction $^{16}\mathrm{O}(\vec{\gamma},\pi^-p)$we use spectroscopic factors of 60% for the *p*-shell orbitals and the *s*-shell orbital, with a harmonic oscillator parameter of $b=1.81$ fm, and for the final state we assume the $p_{3/2}$ orbital is bound by 6.6 MeV and the $s_{1/2}$ orbital is bound by 20 MeV with respect to the ground state of ^{15}O [12].

III. PREVIOUS MEASUREMENTS

Several recent experiments on exclusive pion photoproduction have been reported in the literature. Each one emphasizes different kinematics and energy resolutions. Some experiments average over a large region of kinematics in order to increase statistics, while others choose specific kinematics for high resolution measurements at the expense of full coverage of the angular range.

One of the first experiments of the 1990's was at the Tomsk synchrotron [14]. This measurement of the $^{12}\mathrm{C}(\gamma,\pi^-p)$ reaction at 380 MeV measured only one kinematic setting at a proton angle of 20° and a pion angle of 120° using two spectrometers. The resolution was sufficient to separate proton knock-out from the *s* and *p* shells. These data are in good agreement with calculations [3], however, at backward pion angles the contribution from the Δ resonance to the cross section is very small. These data show that the Born terms and the distorted waves in the theoretical model are reasonably described at energies near the Δ resonances.

The next experiment to be reported was from MIT/Bates [4], where the $^{16}\mathrm{O}(\vec{\gamma},\pi^-p)$reaction at 360 MeV was measured. Two pion angles were chosen, at 64° and 120° , to investigate the sensitivity to the Δ reaction mechanism. The proton detectors were plastic scintillators placed at corresponding angles of 40° and 20° and did not give sufficient energy resolution to determine the knock-out shell state. The low statistics of this measurement required them to average over a large range of pion energies, and still the results had statistical uncertainties of about 50%. Nonetheless, the measured cross sections were a factor of 4 smaller than the calculations at 64°. A possible explanation is that there was a large modification of the ΔN interaction in the nucleus [3]. The large difference between theory and experiment motivated several other laboratories to further explore this reaction.

A more recent experiment has been done at Mainz for the isospin related reaction $^{12}\mathrm{C}(\gamma,\pi^+n)$ at incident photon energies in the range of 250 to 400 MeV [15]. Double differential cross section are reported for neutron knock-out from the *p* shell and are compared with DWIA calculations which are similar to the calculations in Ref. [3]. The surprising result of that work is that the cross sections at forward pion angles are larger than the calculations, in apparent contradiction with the results of Ref. [4]. As a function of photon energy, the cross sections integrated over neutron angle are about a factor of 2 bigger than their calculations at the peak of the delta for forward pion angles. However, we have compared their data with the calculations of Ref. [3] and find agreement within 20–30 %. Either way, these data suggest that the problem with the Bates data [4] is simply due to experimental uncertainties.

Another experiment was done at the LEGS facility at Brookhaven National Laboratory with polarized photons,

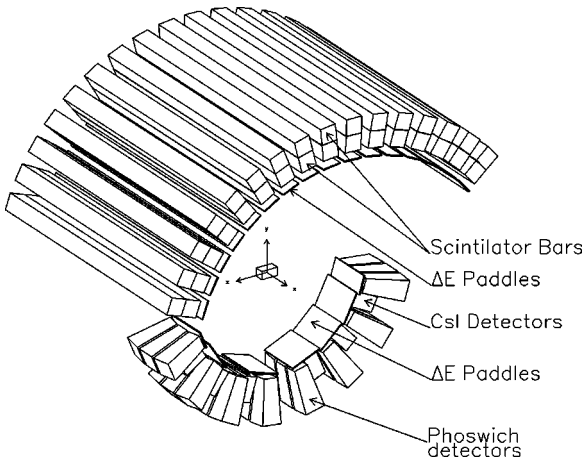

FIG. 1. Schematic drawing of the target and detector setup for the present measurement.

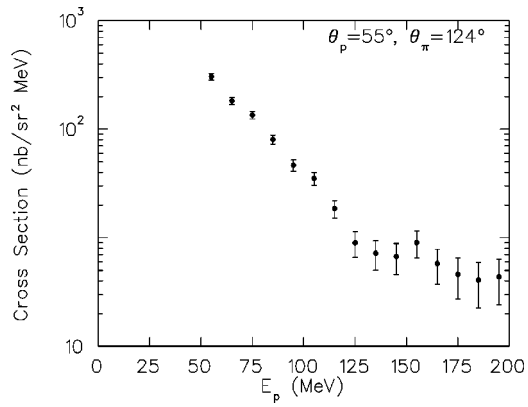

FIG. 2. Triple differential cross sections $d\sigma/(d\Omega_p d\Omega_\pi dE_p)$ as a function of the proton energy E_p without background subtraction. The background at $E_p > 125$ MeV for this angle pair is typical of the background at other angle pairs.

where the spin asymmetries were reported [16]. The spin asymmetries are less sensitive to the absolute normalization errors that can affect the cross section. These data were compared with the calculations of Ref. [3] and within the statistical uncertainties there was no strong evidence for modification of the Δ properties in the nuclear medium.

The AmPS facility at NIKHEF performed a high-resolution study of the $^{16}O(\vec{\gamma},\pi^- p)$ reaction using virtual photons near the bremsstrahlung end point. The electron beam had an energy of 369 MeV and the pion and proton were measured using two spectrometers. They fit the end-point energy spectrum up to 15 MeV in excitation energy. The statistical accuracy of the fits is reflected in the large (20–50 %) error bars on their final cross sections. A comparison of their data with the calculations of Ref. [3] are in good agreement with the local DWIA for both forward and backward pion angles. One advantage of this experiment is that knock-out from the $p_{1/2}$ and $p_{3/2}$ shells can be separated. There may be a small difference in the pion angular distributions for these states as compared with calculations, but the statistical uncertainties are too large to make any definite conclusions.

A summary of these previous experiments is that only one experiment (the one from MIT/Bates) shows a significant deviation from the calculations of Ref. [3], and the more recent experiments with better statistical accuracy and better energy resolution show no strong evidence for modifications of the Δ properties in the nuclear medium. Of course it is well known that the width of the Δ peak becomes larger in the nuclear medium, due in part to the $\Delta N \rightarrow NN$ coupling, but this does not significantly change the observables in the $(\gamma,\pi N)$ reaction [3]. In particular, the ΔN interaction potential in the nucleus remains undetermined.

IV. EXPERIMENTAL DETAILS

The present experiment was done at the Laser Electron Gamma Source (LEGS) facility of the National Synchrotron Light Source (NSLS) of Brookhaven National Laboratory. The linearly polarized photon beam was produced by Compton backscattering of polarized laser light. The Ar-ion laser produced three lines at 364, 351, and 333 nm, which were incident on the 2.58 GeV electrons in the storage ring of the National Synchrotron Light Source, resulting in γ rays with Compton edges at 307, 317, and 332 MeV, respectively. The energy of each photon was known by detecting the scattered electron, which loses energy from Compton scattering and was deflected into a magnetic tagging spectrometer [21] with an energy resolution of $\sigma \simeq 2$ MeV. The energy resolution was limited by the energy spread of the electrons in the storage ring.

The microscopic bunch structure of the electrons in the storage ring was 18.9 ns and a timing resolution of $\sigma \simeq 1.1$ ns was obtained for the $(\gamma,\pi p)$ reaction, measured between the pion detectors and the tagging spectrometer. The photon flux for our experiment was measured by placing a copper sheet, which acts to convert photons to electron-positron pairs, downstream of the target. The converter was placed between two plastic scintillators, where the upstream scintillator served to veto e^+e^- pairs produced before the converter plate. The photon flux was calibrated by placing a large NaI detector directly in the beam during calibration runs at a low laser intensity.

The laser polarization was measured by optics placed after the exit port of the ring dipole (preceeding the laser-electron interaction straight section) thus sampling the laser light that collided with the electron beam. The linear polarization was typically 98% or greater for all measurements. The beam polarization was calculated [22] based on Klein-Nishina scattering using the measured photon energy and the laser polarization. The linear plane of polarization was cycled between orientations parallel and perpendicular to the scattering plane in intervals of roughly 300 s (a random integer was added to the time for each cycle as a precaution). Over the range of photon energies presented here, $E_\gamma = 290$ to 325 MeV, the beam polarization exceeded 95% for both polarization states.

The target was a water-filled cell of dimensions 100 mm long, a width of 57.4 mm and a height of 50.4 mm. The walls of the cell were CH_2 of thickness 0.75 mm on all sides. The

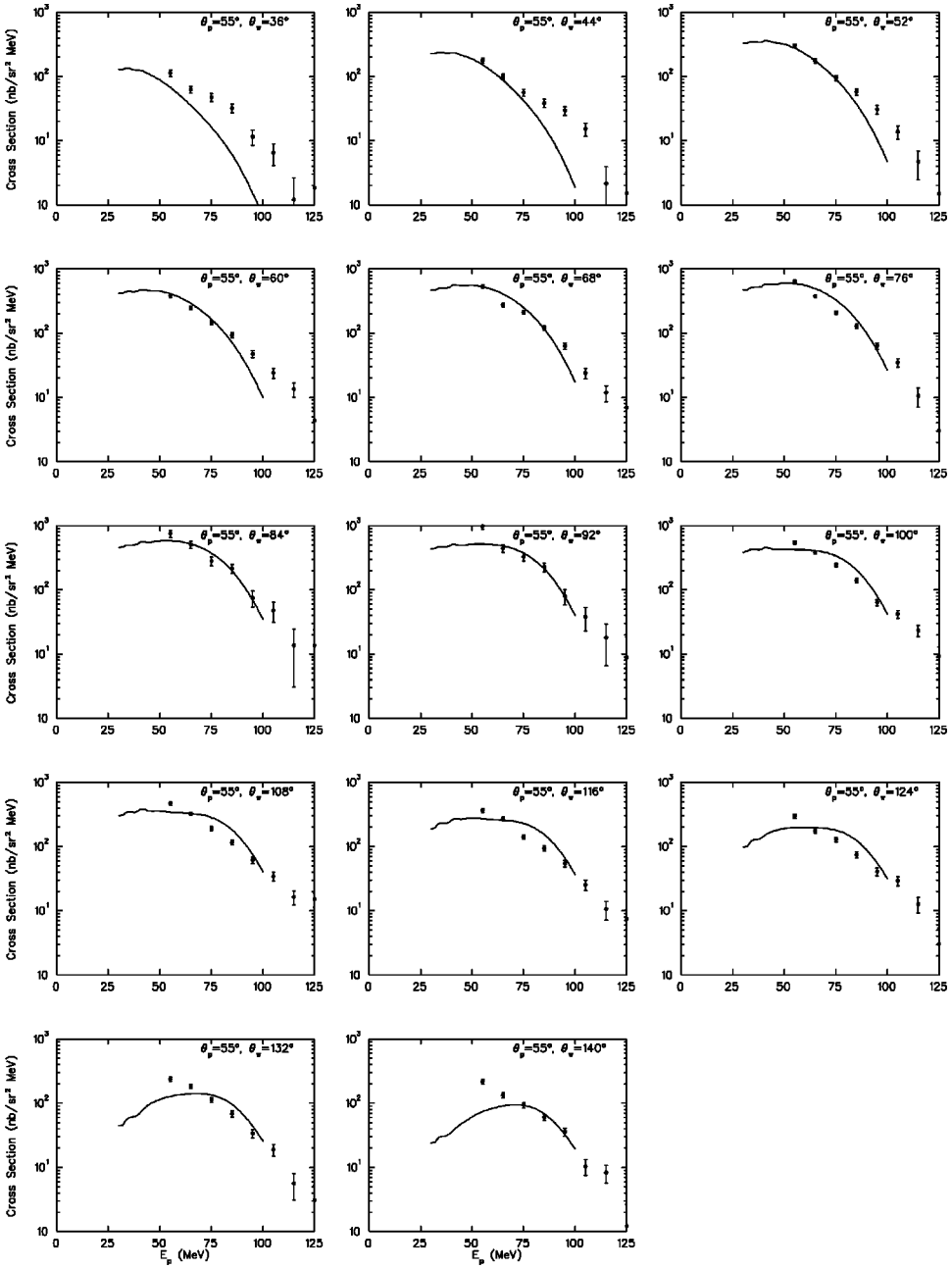

FIG. 3. Same as Fig. 2, except with background subtraction, at all pion angles from 36° to 140° measured in coincidence with a proton at 55°. The theoretical calculations, given by the solid lines, are from the model of Lee, Wright, and Bennhold. All angles are measured in the laboratory frame.

photon beam was collimated to be 20 mm high and 40 mm wide. The target was positioned at the beam center to within 1 mm by using photographic film that was taped to the target and then exposed to the beam. The relative position of the beam was monitored every few hours by a scintillator hodoscope that was placed in the beam between data runs, and remained stable to an accuracy of 1 mm or less. Several empty target runs, where the water was removed from the cell, were done during the course of the experiment in order to do a background subtraction from the cell walls, which contributed only about one percent to the total trigger rate.

Detectors were placed in a cylindrical array surrounding the target. On one side, plastic scintillator bars of length 160 cm and cross sectional area 10 cm by 10 cm were placed in pairs at angles of 20° to 140° in 8° steps at a distance of 105 cm from the target with the length perpendicular to the beam axis, see Fig. 1. These bars were used in a previous experiment in the same geometry (see Ref. [23] for details). A thin ΔE plastic scintillator of 1 cm thickness and 11 cm width was placed just before the bars at a distance of 100 cm from the target. The ΔE paddle was used for charged particle identification by measuring the energy loss of the particle in comparison with the total energy measured by the bars. On the opposite side of the target from the bars, an array of CsI detectors of dimensions 8.9 cm by 8.9 cm and 15.2 cm length were placed at angles of 35° to 135° in 20° steps, except at 95°. The CsI detectors were oriented in pairs side by side, as shown in Fig. 1, with the length aligned radially to the target at a distance of 58 cm to the front face. In addition, thick plastic scintillators of length 26 cm and a radially expanding shape to cover a solid angle of 0.062 sr with the front face at a distance of 58 cm from the target

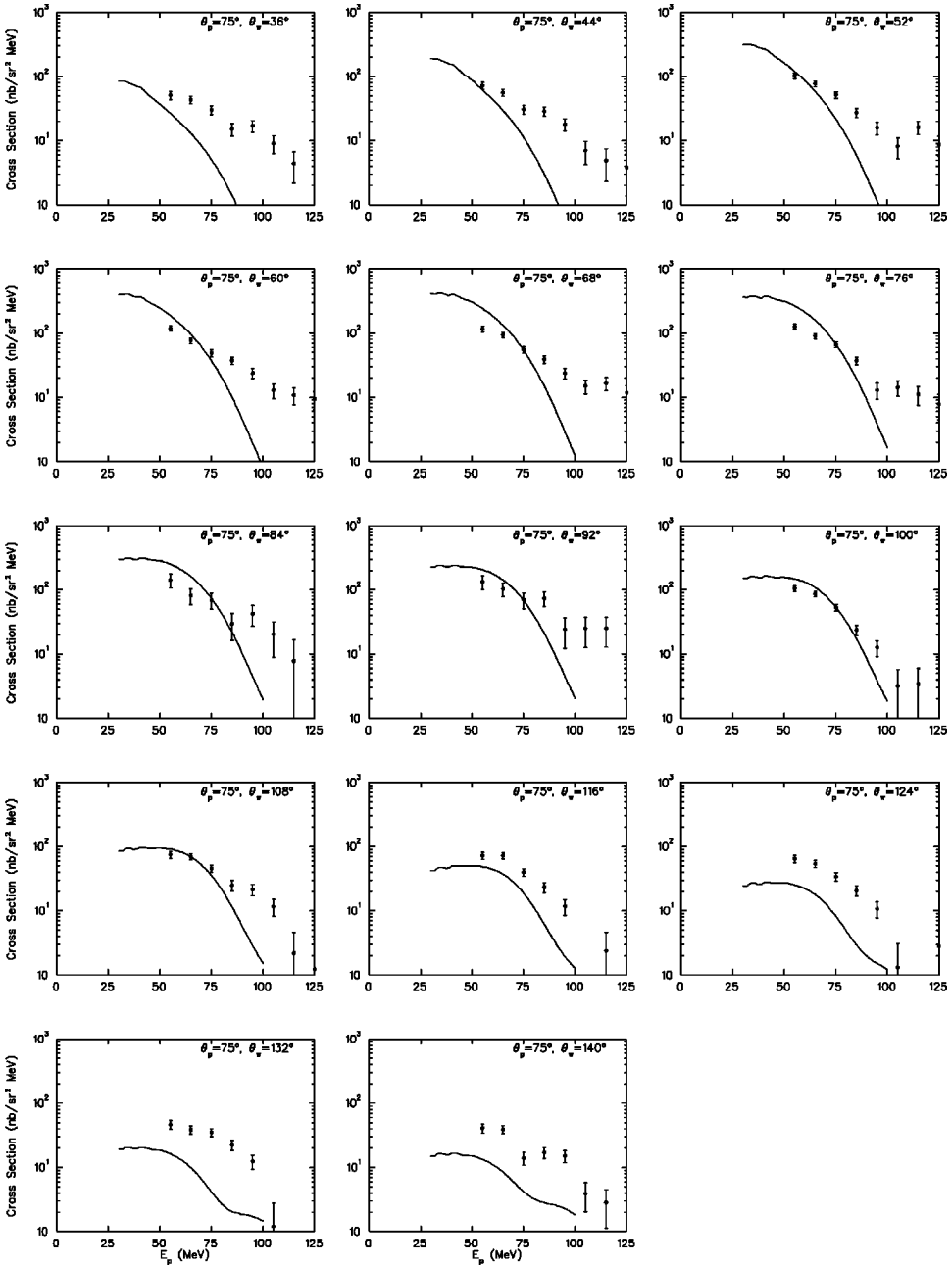

FIG. 4. Same as Fig. 3, except for a proton angle of 75°.

were placed in triplets at each angle as shown in Fig. 1. Thin ΔE plastic scintillators of thickness 6.35 mm were placed just before the CsI and thick plastic detectors for a measurement of energy loss to obtain particle identification.

The light from the scintillators was measured with standard photomultiplier tubes. The pulse height was integrated using ADC (analog to digital) electronics and read into the computer using a modified *Q* data acquisition system. The calibration of pulse height to energy was obtained using deuteron photodisintegration kinematics from calibration runs where the H_2O target was replaced with D_2O. The trigger for all runs was set for a coincidence between any bar on one side and any ΔE on the other side and an electron in the tagging spectrometer. The neutron from deuteron photodisintegration was detected in the bars and the proton was detected in the CsI and thick plastic scintillators for a given tagged photon energy. Energy loss in the target by the proton was modelled by computer simulations which took into account the beam intensity profile incident on the target. The neutron energy was determined from the difference in time between the scintillation detectors and the tagging spectrometer. A missing mass spectrum was calculated from the measured energies and angles of the proton and neutron, along with the photon energy, which provided a test of the energy calibration and helped to eliminate low-energy background. With the energy calibration of the CsI, thick plastics and ΔE scintillators done, the energy calibration of the bars was obtained from $\gamma + n \rightarrow p + \pi^-$ kinematics where the pion was detected in the bars. The events from this reaction on the proton were clearly visible as a peak on top of the three-body kinematics of the oxygen data. Details of the calibration are described in Ref. [24].

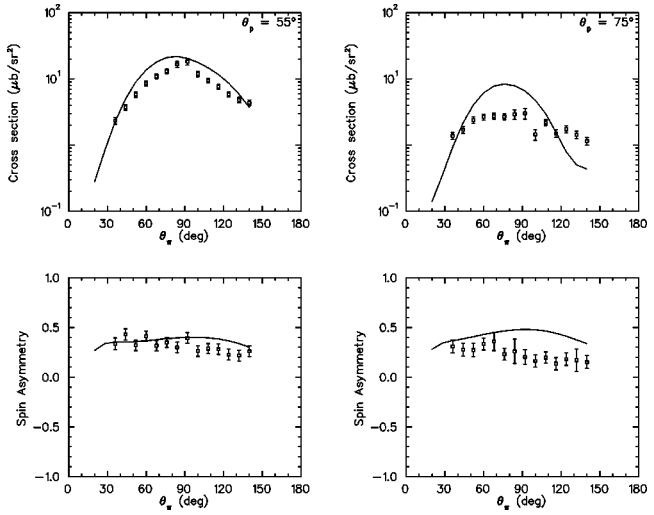

FIG. 5. Double differential cross sections $d\sigma/(d\Omega_p d\Omega_\pi)$ and spin asymmetries $(\sigma_\perp - \sigma_\parallel)/(\sigma_\perp + \sigma_\parallel)$ integrated over the range $E_p = 50$ MeV to 100 MeV, as a function of the pion angle θ_π. The graphs on the left and right correspond to proton angles of 55° and 75°, respectively. The solid lines are the theoretical calculations integrated over the same proton energies.

Absolute cross sections for the oxygen data were obtained from the events where a pion was identified in a ΔE versus E plot of the bars, in coincidence with a proton in the ΔE versus E plot of the CsI or thick plastic detectors, when the relative timing between these events was in the coincidence peak. The beam structure of the electrons in the NSLS storage ring, with ''bunches'' of electrons every 18.9 ns, ensured that coincidence events were separated from the accidental events (where a pion in time with one bunch is detected along with a proton in time with another bunch), even after accounting for the variation in flight time to the detectors. The accidental rate was only 2–3% of the coincidence rate. Accidentals and events from the cell walls, as determined from empty target runs, were subtracted from the yield. Corrections for computer deadtime, typically about 5%, were done for each data run.

The solid angle was taken as the active area of the CsI and thick plastic scintillators on one side, and only the central 40 cm of the bars, as determined by a software cut on the relative timing of the signals from each end of the bars, which is accurate to within a few centimeters. The systematic uncertainty associated with the solid angle in the bars is about 5%. The systematic uncertainty of all other corrections, including target thickness and beam flux normalization, is about 4%, except for the thick plastic scintillators at forward angles of 25° and 45°. For these detectors, the electron-positron pairs from atomic interactions of the photon beam were sufficiently large that the pions could not be cleanly separated in the ΔE-E plot. A similar problem occurred with the bars at forward angles of 20° and 28°. The data from these detectors are not used for the cross sections reported here. However, the spin asymmetry data are not sensitive to the absolute normalization. A software cut on the thick plastic at 45° that retained more than half of the pions and eliminated virtually all electrons in the ΔE-E plot was used, allowing us to calculate the spin asymmetry at this angle. The CsI detectors have better energy resolution and do not suffer from the problem of electron contamination in the identification of pions. For the scintillator bars, the ΔE-E plots for identification of protons were very clean, similar to those shown in the previous work [23].

Because of the thickness of the target, protons of low energy (<30 MeV) generally lost too much energy on the way out of the target and are not useful for the cross section analysis. In addition, protons of energy <50 MeV have efficiency corrections (due to the software threshold on the proton detectors) which introduce large systematic uncertainties. For this reason, we present cross sections only for protons with energies greater than 50 MeV. Similarly, only pion energies greater than 20 MeV are accepted in the bar detectors in order to prevent the cross sections from having unreasonable systematic uncertainties ($>3\%$). The detector efficiencies for both pions and protons were calculated from computer simulations using the GENAT software [17] which includes effects such as pion absorption, pion decay, multiple scattering in the target and other nuclear interactions like proton reactions at low and medium energies. An estimate of the systematic uncertainties for the detector efficiencies depends on the energy of the particles, but is about 5% near threshold (50 MeV for protons and 20 MeV for pions) and about 2% or less at energies above twice threshold.

After applying all of the coincidence requirements and software cuts, some events having protons with energy greater than 150 MeV are still in coincidence with particles in the pion band of the ΔE-E plot. These events are only a small fraction of the total, typically about a few percent, with a roughly uniform distribution in proton energy as shown in Fig. 2. Since the photon energy is around 300 MeV and the mass of the pion is about 140 MeV, we expect few events for the $^{16}\mathrm{O}(\vec{\gamma}, \pi^- p)$ reaction having proton energies above 150 MeV. The origin of these events is uncertain, but it seems likely that these are misidentified pions from the $(\gamma, \pi^+ p)$ reaction [18,19]. The cross sections have been subtracted for this background, assumed uniform in proton energy. This has only a small effect for the cross sections near the peak of the cross section, except at the most forward and backward pion angles where the background subtraction has an effect on the order of 10%. The systematic error associated with this subtraction is 5% at the extreme angles, and typically 1% for most of the data shown in the next section. Taking into account all of the normalization errors and background corrections described above, the overall systematic uncertainty of our cross sections is about 8–12 %, depending on the kinetic energies and angles of the pions and protons detected.

V. RESULTS AND DISCUSSION

Triple differential cross sections as a function of the proton energy are plotted for different pion angles and proton angles of $\theta_p = 55°$ in Fig. 3 and $\theta_p = 75°$ in Fig. 4. The data are presented in this way for direct comparison with the theoretical calculations, because no kinematical averaging is needed. The solid curves are calculated from the theoretical model described in Sec. II, where the photon is assumed to

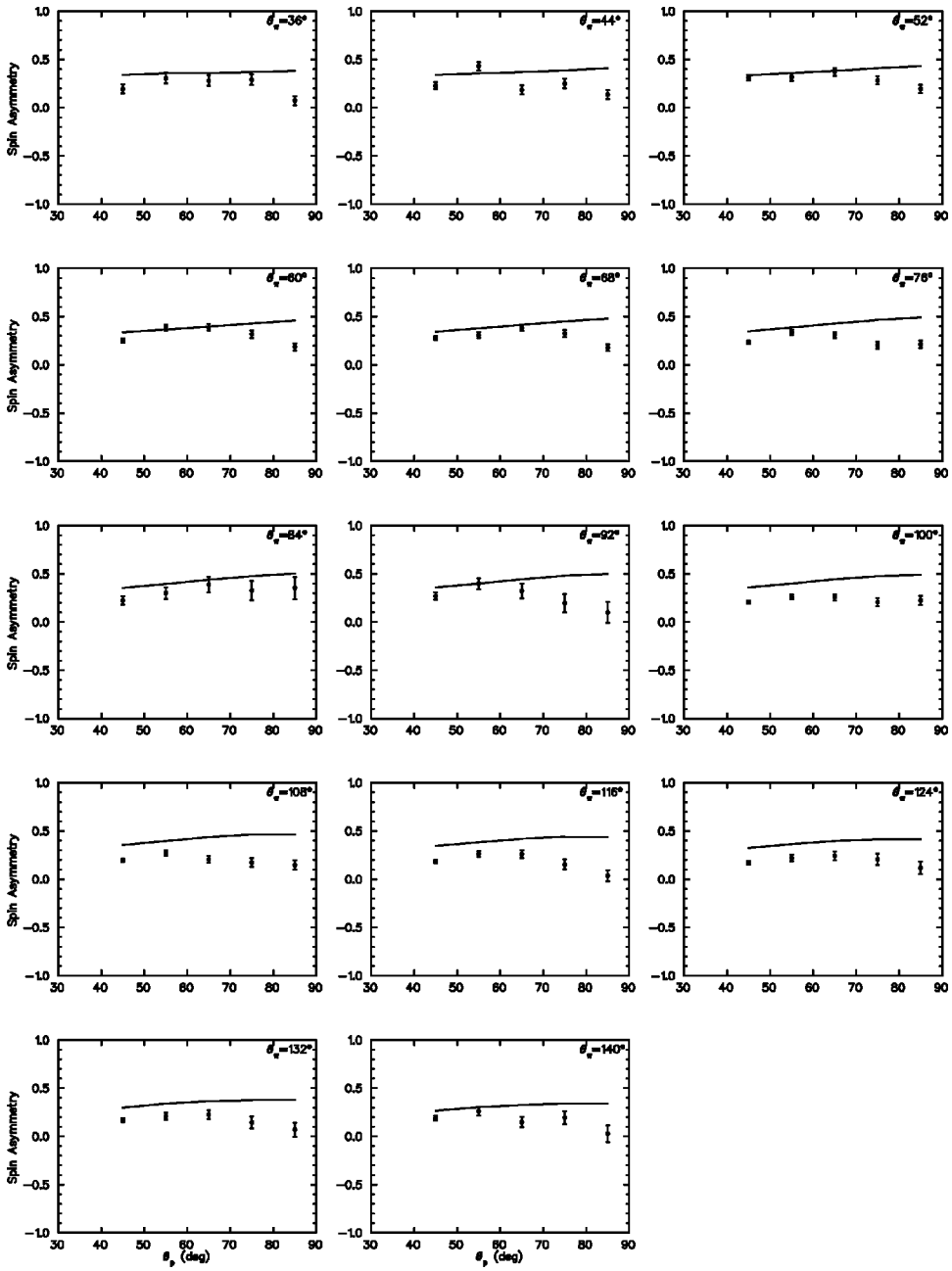

FIG. 6. Spin asymmetries as in Fig. 5, except plotted as a function of the proton angle θ_p, for the pion angles shown in each graph.

interact with any neutron in the oxygen ground state. Note that this is different from Ref. [20] and Ref. [15] where knock-out from only the *p* shell was reported. The data are available in tabular form from Ref. [25].

The calculations have been performed with integrations over the same energy limits corresponding to the particle energy thresholds. This is an important ingredient, because as the proton energy increases, the pion energy decreases and eventually falls below the threshold. There was no cut on missing energy. This cut is sometimes applied [15] in order to restrict the nucleon knock-out to the *p*-shell. The calculations include contributions from *s*-shell knock-out, which account for approximately 10–20 % of the cross section strength.

Comparing the data with the calculations in Fig. 3, we see that the overall agreement is fairly good, except at pion angles of 36° (the most forward angle where pions could be separated from atomic e^+e^- events) and beyond 132° (the most backward angles). Because the contribution from the Δ resonance dominates at forward angles [20], whereas the Born terms are essentially the sole contribution at backward angles, the disagreement between the shape of the theory and the experiment points at pion angles greater than 100° is a bit surprising. A similar trend is seen in the triple differential cross sections of the Mainz data [19], where the data are consistently higher than the distorted wave calculations at higher pion energies (corresponding to lower proton energy). This may reflect the uncertainty in the pion or proton optical potentials at these particular kinematics.

In Fig. 4, the triple differential cross sections are again in reasonable agreement with the theoretical curves except at the most backward angles, where the calculations are a factor

of 3 or more below the data. The cause of the disagreement in Fig. 3 at pion angles greater than 100° is amplified in Fig. 4, where the kinematics are further from the two-body geometry for $\gamma+n\rightarrow p+\pi^-$. The larger momentum transfer (missing momentum) comes from the Fermi motion of the struck nucleon, which is transferred to the recoil momentum of the residual nucleus. The harmonic oscillator wave functions used in the calculations determine the range of the Fermi momentum, and may be suspect at the tail of the distribution where larger Fermi momenta are present. In particular, the Fermi momentum decreases more rapidly for the harmonic oscillator as compared with wave functions that have a Woods-Saxon shape. This may result in a smaller predicted cross section at large pion angles for Fig. 4, although at the momentum transfer in Fig. 3 (which is closer to the two-body kinematics) the harmonic oscillator wave functions should be adequate.

In order to get a better global comparison of the data with the theoretical model, we have integrated the cross sections in the range of proton energies between 50 and 100 MeV and plotted the results in Fig. 5 for both 55° and 75° proton angles. At 55° the calculations are typically in agreement with the data to within 25% over most of the range of pion angles. For this kinematics, we see that a modification of the properties of the Δ resonance in the nuclear medium is not necessary. A similar conclusion has been reached in Refs. [20,15] which is in direct contradiction to the cross sections at forward pion angles reported in Ref. [4]. At $\theta_p=75°$, the shape of the data is much broader than that predicted by the calculations, and the discrepancy is nearly symmetric about a pion angle of 80° or so. This suggests that the problem is not one of medium modifications of the Δ resonance but rather that the harmonic oscillator wave functions are not giving a proper description of the phase space at these kinematics.

The spin asymmetries have already been reported in Ref. [16] although not for the full range of the measurements. For completeness, we have integrated the spin asymmetries over the same region of kinematics as in Fig. 5. The results are also plotted in Fig. 6 as a function of the proton angle θ_p. This plotting format allows for a better comparison with Refs. [15,16]. Figure 6 also includes the data at proton angles of 45° and 65° where the absolute normalization was not possible because of electron contamination (see Sec. IV). These data have smaller error bars than those in Ref. [16] and now one can see more clearly the comparison with theoretical calculations (which have been integrated over $E_p=50$ to 100 MeV to match the present data). In general, the measured spin asymmetries are consistently below the theoretical predictions, especially at proton angles greater than 60°. This provides a stringent test for modifications to the theoretical models, because the spin asymmetries are not sensitive to ambiguities in the theory such as choice of optical potentials or width of the Δ resonance [3]. Modifications to the properties of the Δ resonance, such as approximating the self-energy V_Δ as done in Refs. [3,16], may be necessary to get agreement between the data and calculations. However, the cross sections in Fig. 5 suggest that a better description of the wave function of the struck nucleon are needed before investigating modifications of the Δ.

VI. CONCLUSIONS

The calculations of Lee, Wright, and Bennhold in the framework of the DWIA give a good description of the $^{16}\mathrm{O}(\vec{\gamma},\pi^- p)$ data at kinematics near those of the two-body reaction $\gamma+n\rightarrow p+\pi^-$. At larger proton angles, where the phase space for the two-body reaction is significantly smaller, the pion angular distribution of the data are flatter than predicted by theoretical model and the spin asymmetries are consistently smaller than the calculations.

The cross sections presented here are similar, in comparison to calculations in the same theoretical model, to the cross sections reported by Mainz [15,19] and NIKHEF [20], but disagree with those reported by Bates [4]. The spin asymmetries have smaller uncertainties than those presented earlier [16] and provide a stringent test for theoretical models of pion photoproduction.

ACKNOWLEDGMENTS

The help of the LEGS support staff is greatly appreciated. This work was supported by the National Science Foundation (Grant No. PHY-9722654) and the U.S. Department of Energy under Contract No. DE-AC02-98CH10886.

[1] A. Nagl, V. Devanathan, and H. Überall, *Nuclear Pion Photoproduction* (Springer-Verlag, Berlin, 1991).
[2] G. Blanpied *et al.*, Phys. Rev. C **52**, R455 (1995).
[3] X. Li, L.E. Wright, and C. Bennhold, Phys. Rev. C **48**, 816 (1993).
[4] L.D. Pham *et al.*, Phys. Rev. C **46**, 621 (1992).
[5] R.A. Freedman, G.A. Miller, and E.M. Henley, Nucl. Phys. **A389**, 457 (1982).
[6] K.I. Blomqvist and J.M. Laget, Nucl. Phys. **A280**, 405 (1977); J.M. Laget, **A481**, 765 (1987).
[7] R. Wittman and N.C. Mukhopadhyay, Phys. Rev. Lett. **57**, 1113 (1986).
[8] J.H. Koch, E.J. Moniz, and N. Ohtsuka, Ann. Phys. (N.Y.) **154**, 99 (1984).
[9] R.M. Davidson, N.C. Mukhopadhyay, and R.S. Wittman, Phys. Rev. D **43**, 71 (1991).
[10] K. Stricker, H. McManus, and J. A. Carr, Phys. Rev. C **19**, 929 (1979); **22**, 2043 (1980); **25**, 952 (1982).
[11] P. Schwandt *et al.*, Phys. Rev. C **26**, 55 (1982).
[12] M. Leuschner *et al.*, Phys. Rev. C **49**, 955 (1994).
[13] C.M. Spaltro *et al.*, Phys. Rev. C **48**, 2385 (1993).
[14] P.S. Anan'in and I.V. Glavanakov, Sov. J. Nucl. Phys. **52**, 205 (1990).
[15] J.A. MacKenzie *et al.*, Phys. Rev. C **54**, R6 (1996).
[16] K.H. Hicks *et al.*, Phys. Rev. C **55**, R12 (1997).
[17] GEANT3.2.1, *Detector Description and Simulation Tool*, Applications Software Group, CERN, Geneva, Switzerland.

[18] Liang *et al.*, Phys. Lett. B **411**, 244 (1997).
[19] D. Branford (private communication); J.A. Mackenzie, Ph.D. thesis, Edinburgh University, 1995.
[20] M.A. Uden *et al.*, Phys. Rev. C **58**, 3462 (1998).
[21] C.E. Thorn, G. Giordano, O.C. Kistner, G. Matone, A.M. Sandorfi, C. Schaerf, and C.S. Whisnant, Nucl. Instrum. Methods Phys. Res. A **285**, 447 (1989).
[22] D. Babusci, G. Giordano, and G. Matone, Phys. Lett. B **355**, 1 (1995).
[23] D.J. Tedeschi *et al.*, Phys. Rev. Lett. **73**, 408 (1994); D.J. Tedeschi, Ph.D. thesis, Rensselaer Polytechnic Institute, 1993.
[24] V. Gladyshev, Ph.D. thesis, University of Virginia (unpublished).
[25] Data tables online at NRL http://www.legs.bnl.gov